AAC Journals.ASM.org

# Development of a Population Pharmacokinetic Model Characterizing the Tissue Distribution of Azithromycin in Healthy Subjects

**Songmao Zheng,[a] Peter Matzneller,[b] Markus Zeitlinger,[b] Stephan Schmidt[a]**

Center for Pharmacometrics & Systems Pharmacology, Department of Pharmaceutics, College of Pharmacy, University of Florida, Orlando, Florida, USA[a]; Department of Clinical Pharmacology, Medical University of Vienna, Vienna, Austria[b]

**Recent clinical trials indicate that the use of azithromycin is associated with the emergence of macrolide resistance. The objective of our study was to simultaneously characterize free target site concentrations and correlate them with the $MIC_{90}$s of clinically relevant pathogens. Azithromycin (500 mg once daily [QD]) was administered orally to 6 healthy male volunteers for 3 days. The free concentrations in the interstitial space fluid (ISF) of muscle and subcutaneous fat tissue as well as the total concentrations in plasma and polymorphonuclear leukocytes (PMLs) were determined on days 1, 3, 5, and 10. All concentrations were modeled simultaneously in NONMEM 7.2 using a tissue distribution model that accounts for nonlinear protein binding and ionization state at physiological pH. The model performance and parameter estimates were evaluated via goodness-of-fit plots and nonparametric bootstrap analysis. The model we developed described the concentrations at all sampling sites reasonably well and showed that the overall pharmacokinetics of azithromycin is driven by the release of the drug from acidic cell/tissue compartments. The model-predicted unionized azithromycin (AZM) concentrations in the cytosol of PMLs (6.0 ± 1.2 ng/ml) were comparable to the measured ISF concentrations in the muscle (8.7 ± 2.9 ng/ml) and subcutis (4.1 ± 2.4 ng/ml) on day 10, whereas the total PML concentrations were >1,000-fold higher (14,217 ± 2,810 ng/ml). The total plasma and free ISF concentrations were insufficient to exceed the $MIC_{90}$s of the skin pathogens at all times. Our results indicate that the slow release of azithromycin from low pH tissue/cell compartments is responsible for the long terminal half-life of the drug and thus the extended period of time during which free concentrations reside at subinhibitory concentrations.**

Azithromycin (AZM) is a semisynthetic macrolide antibiotic with a broad range of activity against Gram-positive bacteria and some community-acquired Gram-negative pathogens, including *Haemophilus influenzae* and *Moraxella catarrhalis*, and it is extensively used in the clinic setting for the treatment of respiratory tract infections (1, 2). Compared to the older macrolides, AZM is thought to have advantageous pharmacokinetic (PK) and pharmacodynamic (PD) properties, particularly due to its large distribution volume (~23 liter/kg of body weight) and long half-life of 68 to 79 h (3), which allows for a convenient once-daily dosing regimen and a short overall duration of treatment of 3 to 5 days (4). However, emerging evidence suggests that the use of AZM also triggers the emergence of macrolide resistance (5), but the underlying mechanisms are currently unclear. Particularly alarming data originated from a WHO-recommended mass distribution study conducted in 1,015 Tanzanian children, where the proportion of the total macrolide-resistant *Streptococcus pneumoniae* isolates increased 2- to 3-fold, whereas that of the highly resistant isolates (MIC ≥ 16 μg/ml) was found to be up to 17-fold increased 6 months after a single dose of oral AZM treatment (6).

A closer evaluation of the PK properties of AZM shows that although its large distribution volume suggests extensive tissue distribution, the majority of the drug is confined to intracellular compartments and thus is unavailable for extracellular antimicrobial activity. This is due to the fact that AZM is a diprotic base ($pK_{a1}$, 8.1; $pK_{a2}$, 8.8) (7). Once it enters the acidic compartments, such as the acidic lysosomes of white blood cells, the drug is protonated and trapped inside the cells. This mechanism is widely known as ion trapping and is responsible for the presence of AZM in the tissue long after the administration of the last dose, as reflected by its long elimination half-life of 68 to 79 h (3, 4, 8). While the long presence of AZM in the body is certainly advantageous for exerting its time-dependent bacteriostatic or bactericidal activity at concentrations exceeding the MIC of the pathogen, concerns have been expressed about the long presence of the drug at subinhibitory levels, as they may trigger the development of resistance (9, 10).

It should further be noted that the primary infection site of most bacterial infections is in the extracellular tissue space, i.e., the interstitial space fluid (ISF) (4, 11). Many publications, however, refer to tissue concentrations as drug concentrations obtained from tissue homogenates. This approach is highly misleading, as the concentrations obtained from tissue homogenates represent a mixture of free and total and intra- and extracellular concentrations, making a distinction of how much free drug is in fact available at the infection site difficult. The high AZM concentrations found in white blood cells, different tissue-specific phagocytes, or tissue homogenates from the lung, lymph nodes, prostate, tonsils, and gastric tissue are consequently not representative of the actual target site concentrations (8, 12–17). In order to comprehensively evaluate the potential causes of resistance development against AZM, it is important to assess drug levels not only at the primary infection site, i.e., the lung (especially the epithelial lining fluid [ELF]), but also in other tissues, such as the skin, where microorganisms are available for interaction with AZM and resistance

Received 28 March 2014 Returned for modification 15 June 2014
Accepted 17 August 2014
Published ahead of print 25 August 2014
Address correspondence to Stephan Schmidt, sschmidt@cop.ufl.edu.

doi:10.1128/AAC.02904-14

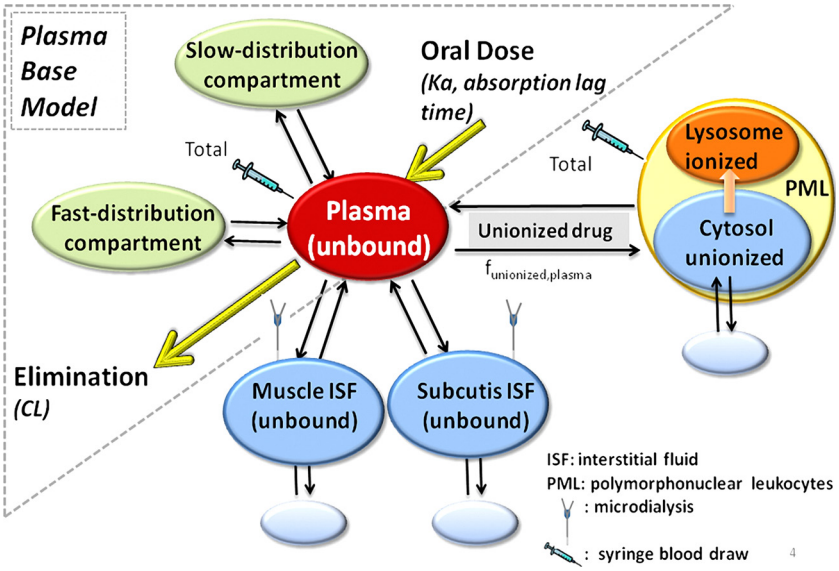


**FIG 1** Model structure of the proposed tissue distribution model for azithromycin.

development. To this end, Matzneller et al. (4) determined the free pharmacologically active concentrations in the ISF of muscle and subcutaneous adipose tissue (subcutis) in a clinical microdialysis study, as well as the total plasma concentrations and total concentrations in polymorphonuclear leukocytes (PMLs) in six healthy male volunteers receiving 500 mg once daily (QD) AZM for 3 days.

The objective of this study was to develop a tissue distribution model for AZM that allows the simultaneous characterization of free drug concentrations in the ISF of muscle and subcutaneous adipose tissue, taking the ionization state at different tissue sites and plasma protein binding into account.

## MATERIALS AND METHODS

**Subjects and pharmacokinetic study.** AZM (500 mg once daily) was administered to 6 healthy male volunteers for 3 days. The total AZM concentrations in plasma were determined at baseline and 0.5, 1, 1.5, 2, 2.5, 3, 3.5, 4, 6, and 8 h after dosing on days 1 and 3, as well as at three defined time points on days 5 and 10 (4). The total concentrations in white blood cells were determined at baseline and 2, 6, and 10 h after dosing on days 1 and 3, as well as at a single time point on days 5 and 10. Free unbound concentrations in the ISF of muscle and subcutaneous adipose tissue were determined via clinical microdialysis at prespecified time points, and the details can be found elsewhere (4).

**Pharmacokinetic model.** A tissue distribution model for AZM (Fig. 1) was developed in a stepwise approach: first, assuming that only free drug is available in the absence of a pH gradient between plasma and tissue fluids (18, 19), the free plasma concentrations were computed by multiplying the total plasma concentrations ($C_p$) by the fraction unbound in plasma ($f_{u,p}$). Given that plasma protein binding is saturable for AZM at therapeutic doses, a concentration-dependent function (cf. equation 1) for $f_{u,p}$ was derived from digitized data (GetData Pty Ltd., Kogarah, Australia) from Bouvier d'Yvoire, Dresco, and Tulkens (20) using GraphPad Prism 5 (GraphPad Software, La Jolla, CA, USA).

$$f_{u,p} = 0.4984 + \frac{0.5339 \times c_p}{230.9 + c_p} \quad (1)$$

Second, a three-compartment model with 1st-order absorption, lag time, and 1st-order elimination was set up to characterize the changes in unbound plasma concentrations over time (Fig. 1). This base model was then expanded in a third step to link changes in the free plasma concentrations over time to the corresponding free tissue concentrations (cf. equation 2), with the concentrations calculated as the ratio of the amount and the respective tissue volume:

$$\frac{dAmount_{(tissue)}}{dt} = k_{in} \times Amount_{(plasma)} - k_{out} \times Amount_{(tissue)} + k_{off} \times Amount_{(tissue,deep)} - k_{on} \times Amount_{(tissue)} \quad (2)$$

where $k_{in}$ and $k_{out}$ are the first-order rate constants describing the distribution of AZM in and out of the tissue, respectively. Given the affinity of protonated AZM to negatively charged phospholipids (21, 22), we compared the model performances with or without the inclusion of unspecific binding in PMLs and tissues [amount represented by $Amount_{(tissue,deep)}$], where drugs bind with a first-order rate constant, $k_{on}$, and become available again for distribution with a first-order rate constant, $k_{off}$. At steady state, the amount of drug going into the tissue is equal to the amount of drug coming out of the tissue, as shown in equation 3.

$$k_{in} \times Amount_{(plasma)} = k_{out} \times Amount_{(tissue)} \quad (3)$$

Converting amounts into the corresponding concentrations by accounting for the respective distribution volumes and rearranging for concentrations in tissue ($C_{tissue}$) yields the following expression:

$$C_{tissue} = \frac{Amount_{(tissue)}}{V_{tissue}} = \frac{Amount_{(tissue)} \times k_{out} \times C_{tissue}}{k_{in} \times C_{plasma} \times V_{plasma}} = \frac{Amount_{(tissue)} \times k_{(out)} \times DF_{tissue}}{k_{in} \times V_{plasma}} \quad (4)$$

where $DF_{tissue}$ is a tissue distribution factor accounting for tissue-specific differences in the drug concentrations available for distribution with respect to plasma (cf. equation 5).

$$DF_{tissue} = \frac{C_{tissue}}{C_{plasma}} \quad (5)$$

For this analysis, three tissue distribution factors were defined, one for muscle ($DF_{muscle}$), one for subcutis ($DF_{subcutis}$), and one for the cytosol of PMLs [$DF_{PML(cytosol)}$]. In the absence of a pH gradient, e.g., between plasma and the ISF of muscle and subcutaneous adipose tissue under noninflammatory conditions, this tissue distribution factor approximates the ratio of free unbound drug concentrations between tissue and plasma,

whereas the ionization state of AZM needs to be considered in the presence of a pH gradient. The respective unionized fraction ($f_{unionized}$), which takes the two $pK_a$ values of AZM into consideration ($pK_{a1}$, 8.1; $pK_{a2}$, 8.8), can be computed according to equation 6 (23).

$$f_{unionized} = \frac{1}{1 + 10^{(pK_{a1} - pH)} + 10^{(pK_{a1} - pH) + (pK_{a2} - pH)}} \quad (6)$$

$DF_{PML(cytosol)}$ can consequently be computed as in equation 7:

$$DF_{(PML(cytosol))} = \frac{c_{PML(cytosol,unionized)}}{c_{plasma(uniomized)}} = \frac{c_{PML(cytosol,total)} \times f_{unionized,PML\ cytosol}}{c_{plasma(unbound)} \times f_{unionized,plasma}} \quad (7)$$

where $C_{PML(cytosol,unionized)}$ is the unionized concentration in the cytosol of PMLs, $C_{plasma(unionized)}$ is the unionized concentration in plasma, $C_{PML(cytosol,total)}$ is the total concentration in PMLs, $C_{plasma(unbound)}$ is the free concentration in plasma, $f_{unionized,PML(cytosol)}$ is the fraction unionized in the cytosol of PMLs, and $f_{unionized,plasma}$ is the unionized fraction in plasma. Equation 6 can also be used to compute the differences in $f_{unionized}$ in different cell compartments, e.g., between the cytosol of PMLs (pH ~7 [23, 24]) and the lysosomes located within PMLs (pH ~5 [23, 25]). Given that $f_{unionized}$ in the lysosomes is very low (0.000013), we assumed that once AZM is protonated in the acidic environment of lysosomes, it is trapped and thus no longer available for direct exchange with the plasma compartment.

The total AZM concentrations in PMLs ($C_{PML,total}$) are the sum of the total amounts in the cytosol and lysosomes of PMLs divided by the total PML volume. Provided that approximately one-third of the drug resides in the cytosol of PMLs (26) and that the respective volume ratio between the lysosomes [$V_{PML(lysosome)}$] and cytosol [$V_{PML(cytosol)}$] is 5:95 for macrophages (27) and fibroblasts (28), the ratio between the total AZM concentrations in the cytosol of PMLs [$C_{PML(cytosol,total)}$] and total AZM concentrations in PML($C_{PML,total}$) is computed according to equation 8.

$$\frac{c_{PML(cytosol,total)}}{C_{PML,total}} = \frac{C_{PML(cytosol,total)}}{\left(\frac{Amount_{(PML)}}{V_{PML(lysosome)} + V_{PML(cytosol)}}\right)} = \frac{C_{PML(cystol,total)}}{\left(\frac{3 \times C_{PML(cytosol,total)} \times V_{PML(cytosol)}}{V_{PML(lysosome)} + V_{PML(cytosol)}}\right)} = \frac{1}{3} \times \left(1 + \frac{V_{PML(lysosome)}}{V_{PML(cytosol)}}\right) \quad (8)$$

$C_{PML(cytosol,total)}$ is computed according to equation 9.

$$c_{PML(cytosol,total)} = \frac{1}{3} \times \left(1 + \frac{V_{PML(lysosome)}}{V_{PML(cytosol)}}\right) \times C_{PML,total} = \frac{1}{3} \times \left(1 + \frac{5}{95}\right) \times C_{PML,total} \approx 0.351 \times C_{PML,total} \quad (9)$$

The free unionized concentrations in the cytosol of PMLs [$C_{PML(cytosol,unionized)}$] is computed according to equation 10.

$$C_{MPL(cytosol,unionized)} = C_{PML(cytosol,total)} \times f_{unionized,PML\ cytosol} \quad (10)$$

Similar relationships can be used to compute the total concentrations in the lysosomes of PMLs [$C_{PML(lysosome,total)}$ (cf. equation 11)].

$$C_{PML(lysosome,total)} = \frac{2}{3} \times \left(1 + \frac{V_{PML(cytosol)}}{V_{PML(lysosome)}}\right) \times C_{PML,total} \approx 13.33 \times C_{PML,total} = 38 \times C_{PML(cytosol,total)} \quad (11)$$

We also tested a volume ratio of 1:200 between the lysosome and cytosol, as reported for liver cells (29), but a sensitivity analysis suggested that the resulting changes in the $C_{PML(cytosol)}$-to-$C_{PML,total}$ ratio were marginal (0.351 for the 5:95 ratio versus 0.335 for the 1:200 ratio) and did not significantly improve the overall model fit. However, a volume ratio of 1:200 will affect the concentration ratio between $C_{PML(lysosome,total)}$ and $C_{PML,total}$.

The population pharmacokinetic (pop-PK) model was built in NONMEM version 7.2.0 (Icon, Dublin, Ireland) using the ADVAN13 subroutine and the first-order conditional estimation with interaction (FOCEI) method. The objective function value computed by NONMEM was used in a log-likelihood ratio test for the comparison of hierarchical models. The addition of a structural or variance parameter was considered statistically significant when the objective function value dropped by ≥3.84 ($P < 0.05$ for 1 degree of freedom). Interindividual variability was modeled by an exponential error model, found in equation 12, which assumes a log-normal distribution:

$$P_i = P_p \times e^{\eta i} \quad (12)$$

where $P_p$ is the population value for the parameter P, $P_i$ is the value for this parameter for the $i$th individual, and $\eta_i$ is the interindividual random variability, which is assumed to be normally distributed, with a mean of 0 and variance $\omega^2$. The difference between the observed and model-predicted concentrations was modeled as an additive ($\varepsilon_{add,ij}$) and proportional ($\varepsilon_{prop,ij}$) error, as in equation 13:

$$y_{obs} = y_{pred}(1 + \varepsilon_{prop,ij}) + \varepsilon_{add,ij} \quad (13)$$

where $\varepsilon_{ij}$ is the residual error, with mean 0 and variance $\omega^2$, between the $j$th observation in the $i$th individual ($y_{obs}$) and its model-based prediction ($y_{pred}$). Due to the limited number of subjects ($n = 6$) and the relatively homogeneous study population (all healthy males; age, 29.0 ± 9.63 years; weight, 77.68 ± 8.56 kg; height, 184.17 ± 6.74 cm; body mass index, 22.83 ± 1.39 kg/m$^2$ [all values mean ± SD] [4]), a rigorous covariate analysis was deemed meaningless for this study. In addition to the statistical and graphical evaluations, physiological meaningfulness was considered imperative in the assessment of the model structure and the goodness-of-fit. The robustness of the final model and its parameter estimates were evaluated using a nonparametric bootstrap with 1,000 runs in PLT Tools (version 2.6; PLTsoft, San Francisco, CA) for NONMEM. The graphics were created by ggplot2 libraries for R (version 3.0.1) and GraphPad Prism 5.

## RESULTS

The total AZM concentrations during and after treatment were highest in white blood cells due to intracellular accumulation, whereas the respective total concentrations in plasma and the free concentrations in the ISF of muscle and subcutis were markedly lower. In comparison, the calculated free and unionized AZM concentrations in the cytosol of PMLs (6.0 ± 1.2 ng/ml) were similar to the measured unbound concentrations in the ISF of muscle (8.7 ± 2.9 ng/ml) and subcutis (4.1 ± 2.4 ng/ml) on day 10. When taking pH differences between plasma and cell compartments into consideration, we showed that AZM is almost completely protonated in the acidic environment of the lysosomes of the PMLs ($f_{unionized}$, 0.000013), whereas it is less protonated in the cytosol of the PMLs ($f_{unionized}$, 0.0012). In plasma and the ISF of soft tissues, the $f_{unionized}$ was calculated as 0.0076 due to the absence of significant pH differences between both tissues. These differences in $f_{unionized}$ values reflect the pH gradients between the extracellular milieu (plasma) and the cytosol (about 0.4 pH units) or the lysosomes (about 2 to 2.4 pH units). Our calculations further indicate that the unionized concentrations in the lysosome and cytosol of PMLs appeared to be in the same range (6.0 ± 1.2 versus 2.5 ± 0.5 ng/ml) on day 10.

A model consisting of sampling and distribution compartments in the plasma and soft tissues, as well as a pH-driven distribution compartment in PMLs (Fig. 1), fit the experimentally determined AZM concentrations in plasma, PMLs, and the ISF of

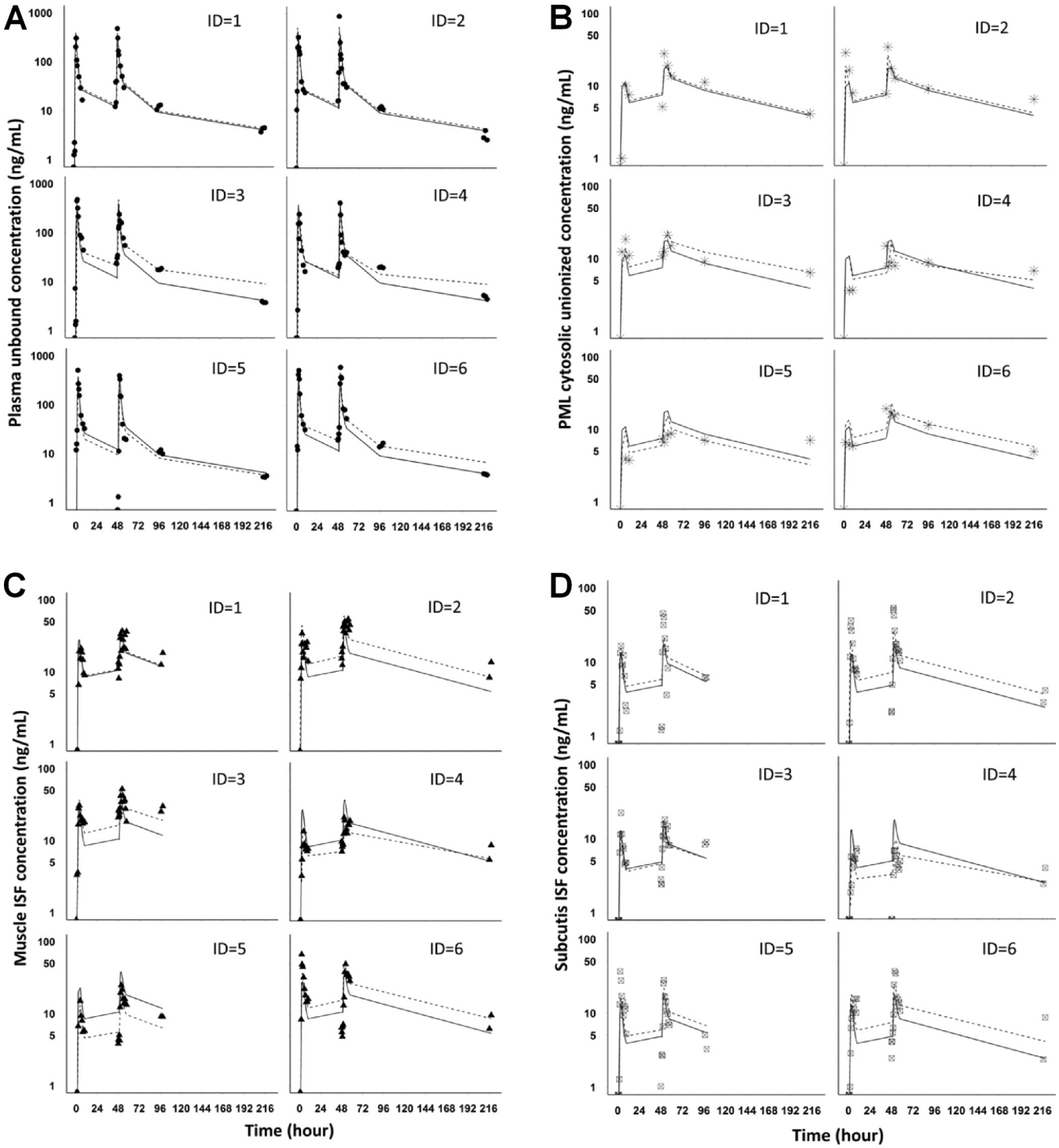


**FIG 2** Observed data and simultaneous model fitting for azithromycin in plasma (unbound) (A), PML (cytosolic unionized) (B), muscle (C), and subcutis ISF (unbound) (D) for assessment of the goodness of model fit. The symbols represent clinically measured concentrations, the solid lines represent model-predicted concentrations on a population level, and the dashed lines represent model-predicted concentrations on an individual level. ID, identification no.

muscle and subcutaneous adipose tissue on the individual subject level (Fig. 2), as well as the population level (Fig. 3) reasonably well. Visual inspection of the goodness-of-fit plots also did not reveal any model misspecification (Fig. 4). The model parameter estimates obtained from a single estimation run are overall in good agreement with the respective bootstrap values, except for the peripheral distribution volume (Table 1), which is likely due to the small sample size and the relatively high variability in the data. Nevertheless, our model-predicted parameter values for plasma are consistent overall with those previously reported in the litera-

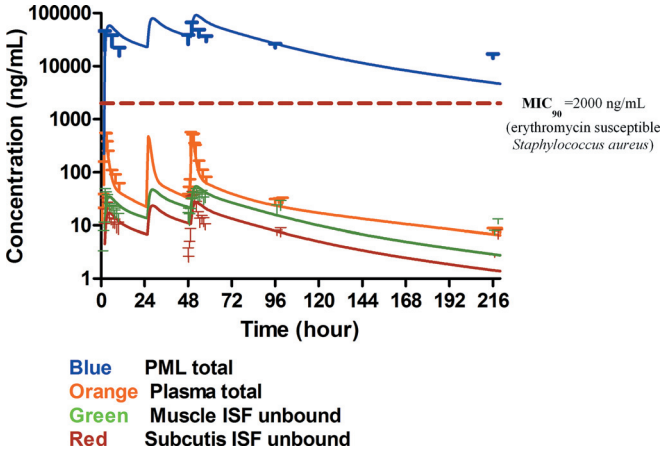


**FIG 3** Model predicted time-mean concentration profile of azithromycin (solid lines) versus observed mean values (symbols) in plasma (total), PMLs (total), and the interstitial space fluid of muscle and subcutis (both unbound).

ture for healthy subjects (30, 31). Our findings further show that the tissue distribution factor for PMLs ($DF_{PML(cytosol)}$, 52) is significantly higher than the corresponding values for muscle ($DF_{muscle}$, 0.55) and subcutis ($DF_{subcutis}$, 0.25), as would be expected, reflecting the differences in the extent of distribution into these tissues. The computed differences in the distribution factors are also reflective of the differences in the pH-mediated ionization state, which plays a major role in the distribution and accumulation of AZM in tissues. Our findings further indicate that there is significant nonspecific binding to tissues, as the inclusion of the additional distribution compartment with the same $k_{on}$ ($0.56\ h^{-1}$) and $k_{off}$ ($0.05\ h^{-1}$) values for the different tissue sites significantly improved the fit of the model to the data.

When linking the model-predicted mean area under the concentration-time curve (AUC) values to the $MIC_{90}$ of clinically relevant skin pathogens (e.g., erythromycin-susceptible *Staphylococcus aureus*, with $MIC_{90}$, 2 μg/ml [32]), the total $AUC_{0-24}/MIC_{90}$ ($AUC_{0-24}$, area under the concentration-time curve from 0 to 24 h) ratios in plasma and in the ISF of muscle and subcutis were <2, while the ratios in PMLs were >50 throughout the sampling period (Fig. 3). On day 10, the $AUC_{0-24}/MIC_{90}$ ratios fell to <0.1, based on predicted plasma and tissue ISF concentrations.

## DISCUSSION

Resistance to antibiotics is a major public health problem, as it leaves physicians with few or no drug choices to effectively treat patients (5, 33). A number of studies have shown that the primary reason for the development of drug resistance is the use of antimicrobials (34), even when an antibiotic is used at the recommended dose for the approved therapeutic indication(s). In recent years, this has become particularly evident for macrolide antibiotics (6, 35–37), where, for example, Malhotra-Kumar et al. (5) clearly demonstrated in a randomized, double-blind, and placebo-controlled study that following a single course of AZM, macrolide resistance increased by up to 60% and remained 14% higher even at 6 months after the end of drug therapy compared to that with the placebo. In order to better understand the pharmacokinetic/pharmacodynamic reasons behind this drug-induced increase in antimicrobial resistance, Matzneller et al. (4) determined the concentration-time course of AZM plasma (total), PMLs (total), and in the ISF of potential infection sites (muscle and subcutaneous adipose tissue) following three consecutive doses of 500 mg QD in healthy volunteers. Their findings confirmed that AZM accumulates in white blood cells, but they also showed that the respective free unbound soft tissue concentrations were markedly lower, resulting in subtherapeutic levels. The objective of our study was to develop a tissue distribution model that allows the simultaneous characterization and prediction of the concentration-time profiles of AZM in plasma, PMLs, and the ISF of muscle and subcutaneous adipose tissue by accounting for the differences in ionization at physiological pH values in the different tissues.

The findings of our study show that the dibasic nature of AZM plays a major role in its distribution into the tissues and explains its accumulation in acidic compartments of, for example, white blood cells, resulting in total cell concentrations that are >1,000-fold higher than the respective total concentrations in plasma. In particular, our calculation of AZM accumulation ratios in the subcellular compartments of PMLs are in agreement with the ratios predicted using another subcellular disposition model (23). In addition to the pH-dependent accumulation of AZM in acidic cell compartments, it has also been shown that the drug can bind in its protonated form to negatively charged phospholipids, which further increases its accumulation in tissues (22, 38). We accounted for this phenomenon by testing an additional distribution compartment for each of the tissues, i.e., muscle, subcutaneous adipose tissue, and PMLs, into which drug enters at a first-order rate, $k_{on}$, and from which it is released at a first-order rate, $k_{off}$. Significant improvement in the overall model fit for all tissues suggests that the inclusion of such a nonspecific tissue distribution compartment is necessary to appropriately account for the tissue distribution kinetics of AZM. The slow release of AZM from these tissue compartments, particularly from the acidic cell compartments, is responsible for its long terminal half-life of about 68 to 79 h (3) after multiple dosing and explains why it is still detectable 172 h after the last dose (4). Findings in the literature suggest that this long terminal half-life is associated with the turnover of neutrophils (half-life [$t_{1/2}$], ~90 h in the uninfected state) (39), provided that ~50 to 70% of the drug is trapped in the lysosomes at steady state, suggesting that it is almost completely unavailable for immediate back-distribution to the plasma. These findings are consistent with the results from *in vitro* assays, which show that cell-associated drug is released only slowly (7, 26). AZM, which is trapped within acidic cell compartments, consequently becomes available for clearance once the cell structural area is broken down during the natural turnover of white blood cells. In other words, the rate at which the drug is released from these cell compartments drives the kinetics of AZM in the terminal phase of the concentration-time profile. The fact that our calculated unionized concentrations in the lysosome and cytosol of PMLs are in the same range on day 10, i.e., the terminal elimination phase, further suggests that equilibrium exists between different subcellular compartments within the PMLs, as was discussed for the distribution of AZM between different tissue compartments (7, 26).

While the long terminal half-life of AZM certainly helps to maintain drug concentrations above the MIC of the infecting pathogen following drug administration in certain compartments, it is also responsible for exposing pathogens to subinhibitory concentrations for a very long time once concentrations drop below the respective susceptibility breakpoints. The data from Matzneller et al. (4) suggest that the total concentrations in plasma

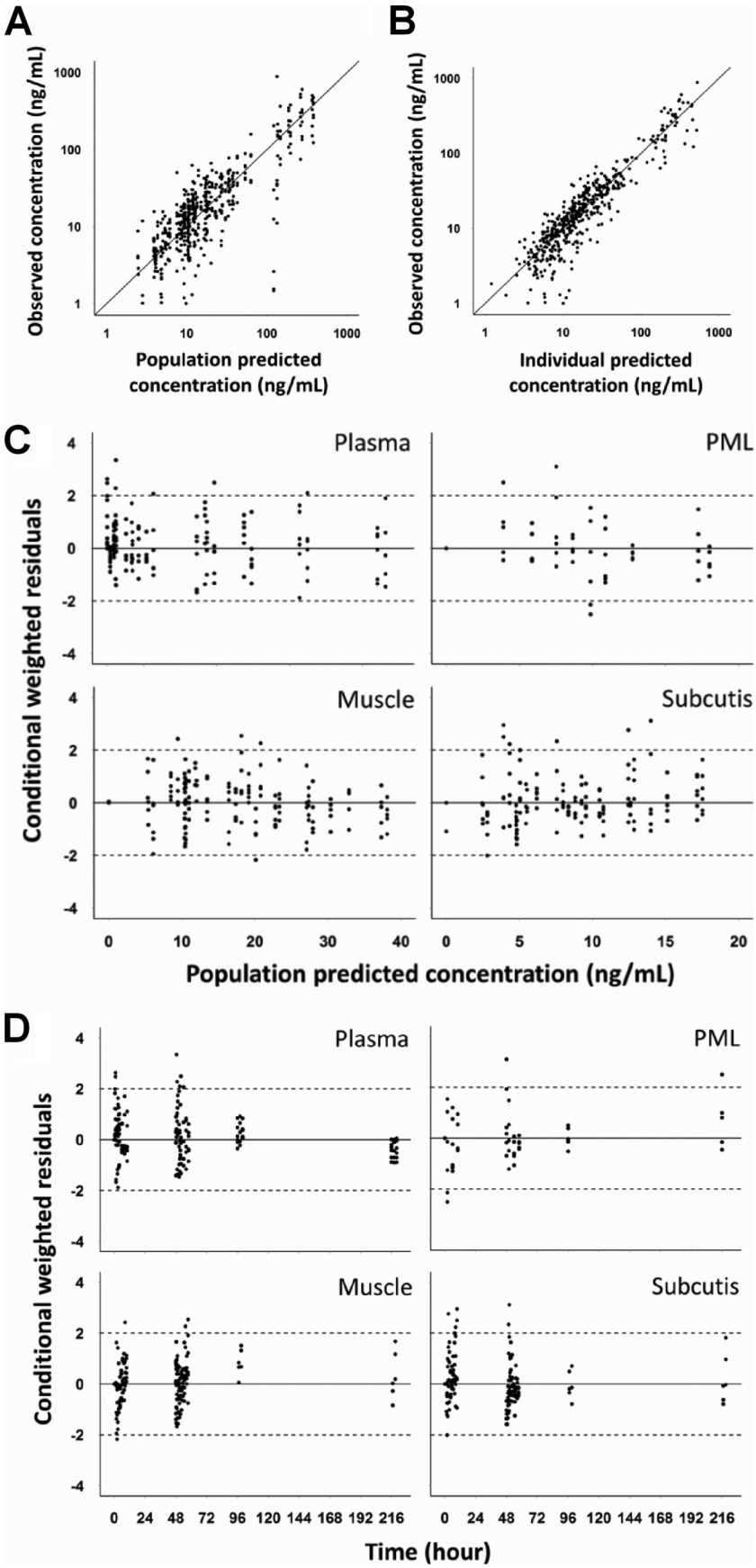


**FIG 4** Goodness-of-fit plots for the pharmacokinetic model of azithromycin observed versus population predicted concentration (A), observed versus individual predicted concentration (B), conditional weighted residuals versus population predicted concentration (C), and conditional weighted residuals versus time (D).

**TABLE 1** Parameter estimates and bootstrap values[a]

| Parameter[b] | Single run | Bootstrap (median)[c] | SE[d] | 95% CI[e] |
|---|---|---|---|---|
| Fixed-effects parameters | | | | |
| $T_{lag}$ (h) | 1.45 (fixed) | 1.50 | 0.34 | (1.07, 2.45) |
| $k_a$ ($h^{-1}$) | 0.88 (fixed) | 0.88 | 0.60 | (0.61, 1.72) |
| CL/F (liters/h) | 258 (fixed) | 227 | 115 | (71, 517) |
| $V_c$/F (liters) | 160 | 240 | 561 | (4.1, 1,790) |
| $V_{P1}$/F (liters) | 1,190 | 1,737 | 38,783 | (262, 4,643) |
| $Q_{P1}$/F (liters/h) | 207 | 208 | 82 | (76, 389) |
| $V_{P2}$/F (liters) | 9,721 | 4,899 | 16,396 | (84, 20,359) |
| $Q_{P2}$/F (liters/h) | 101 | 100 | 55 | (1.2, 214) |
| $k_{in}$ ($h^{-1}$) | 0.16 | 0.14 | 0.29 | ($9 \times 10^{-8}$, 0.8) |
| $k_{out}$ ($h^{-1}$) | 0.15 | 0.10 | 0.05 | (0.02, 0.21) |
| $k_{on}$ ($h^{-1}$) | 0.56 | 0.43 | 0.19 | (0.18, 0.99) |
| $k_{off}$ ($h^{-1}$) | 0.05 | 0.04 | 0.03 | (0.01, 0.10) |
| $DF_{muscle}$ | 0.55 | 0.67 | 0.70 | (0.35, 3.10) |
| $DF_{subcutis}$ | 0.25 | 0.37 | 0.42 | (0.14, 1.64) |
| $DF_{PML(cytosol)}$ | 52 | 63 | 93 | (39, 423) |
| Interindividual variability (%) | | | | |
| $T_{lag}$ | 17.6 | 18.6 | 8.6 | (2.8, 31.1) |
| CL/F | 29.3 | 22.4 | 45.8 | (1.1, 64) |
| $V_{central}$/F | 168.3 | 79.6 | 1,017 | (1.6, 1,804) |
| $k_{in}$ | 0.22 | 22.4 | 3,473 | (0.2, 184) |
| $DF_{muscle}$ | 26.9 | 26.8 | 27.0 | (8.0, 139) |
| $DF_{subcutis}$ | 31.5 | 31.5 | 69.8 | (1.8, 235) |
| $DF_{PML(cytosol)}$ | 0.22 | 9.0 | 35.6 | (0.2, 174) |
| Residual variability | | | | |
| Plasma (proportional) | 0.14 | 0.13 | 0.74 | (0.08, 0.22) |
| Plasma (additive) | 35.2 | 30.4 | 22.7 | (7.2, 94.9) |
| Muscle ISF (proportional) | 0.14 | 0.14 | 0.05 | (0.05, 0.24) |
| Muscle ISF (additive) | 0.51 | 0.38 | 0.49 | ($1 \times 10^{-6}$, 1.37) |
| Subcutis ISF (proportional) | 0.34 | 0.34 | 0.09 | (0.21, 0.54) |
| Subcutis ISF (additive) | $1 \times 10^{-6}$ | $1 \times 10^{-6}$ | 0.002 | ($1 \times 10^{-6}$, 0.008) |
| PML cytosol (proportional) | 0.23 | 0.23 | 0.09 | (0.12, 0.48) |
| PML cytosol (additive) | $1 \times 10^{-6}$ | $1 \times 10^{-6}$ | 0.003 | ($1 \times 10^{-6}$, 0.009) |

[a] $n = 1{,}000$.

[b] Since the unbound concentrations in plasma did not equal the measured unbound concentrations in tissue ISF, a parameter termed the distribution factor for the tissue ($DF_{muscle}$, $DF_{subcutis}$, or $DF_{PML(cytosol)}$) was introduced. $k_a$, first-order absorption rate constant; $T_{lag}$, lag time for absorption; CL/F, apparent clearance; $V_c$/F, apparent volume of the central compartment; $V_{P1}$/F, apparent volume of the fast equilibrating peripheral compartment; $Q_{P1}$/F, intercompartmental distributional clearance of fast equilibrating compartment; $V_{P2}$/F, apparent volume of the slow equilibrating peripheral compartment; $Q_{P2}$/F, intercompartmental distributional clearance of slow equilibrating compartment; $k_{in}$, rate constant for unbound AZM uptake into tissue ISF or for unionized AZM in plasma uptake into PML; $k_{out}$, rate constant for the reverse process described for $k_{in}$; $k_{on}$ and $k_{off}$, on and off rate constants, respectively, for nonspecific tissue binding in the tissue/PML.

[c] The bootstrap results for the $T_{lag}$, $k_a$, and CL/F fixed parameter estimates were based on bootstrap ($n = 1{,}000$) for unbound plasma only.

[d] SE, standard error determined as the standard deviation (SD) of the bootstrap parameter distribution.

[e] 95% CI, 95% confidence interval computed as the 2.5th and 97.5th percentiles of the bootstrap parameter distribution.

are sufficient to exceed the previously proposed $AUC_{0-24}/MIC_{90}$ value of 25 (40–42) for highly susceptible ($MIC_{90} \leq 0.125$ μg/ml) lung pathogens, such as erythromycin-susceptible *S. pneumoniae*. However, the concentrations in both the plasma and ISF of muscle and subcutaneous adipose tissue are insufficient to prevent infections with skin pathogens, such as *S. aureus*, at any point in time. These findings suggest that treatment with 500 mg QD oral AZM is insufficient to treat many skin and skin structure infections. Insufficient AZM concentrations in other tissues, such as the pharynx, where lung pathogens are located, may also contribute to off-target site emergence of resistance and/or to resistance development in bystander organisms.

It should be noted, however, that the concentration-time profiles of this study were obtained from healthy volunteers and are unlikely to accurately reflect disease conditions. This is due to the fact that chemotactic drug delivery is an important determinant for drug exposure in infected tissues, as phagocytes migrate to the infection site and increase local drug concentrations by releasing AZM from their lysosomes (43). In spite of being trapped inside the lysosomal compartments of white blood cells (WBCs) or fibroblasts (44–47), AZM retains its antimicrobial properties and, once released, is available for antimicrobial activity at the infection site (48, 49). It has also been shown that the local pH values in the ISF can be reduced, due to the metabolic activities of infiltrating neutrophils (anaerobic glycolysis) and infecting pathogens (e.g., production of short-chain fatty acids [50, 51]), which result in a further increase in local ISF concentrations. The relevance of this mechanism was demonstrated in several animal and clinical studies by showing that free AZM exposure in infected tissues was significantly higher than that in noninfected tissues (52). Ballow et

al. (30) reported that the median PML count in the cantharidin-induced inflammatory blisters was about 10 times higher than that in the suction-induced noninflammatory blisters in healthy subjects. As a consequence, the mean AZM AUC in the inflammatory blisters was 2.2 times higher than that in the noninflammatory blisters, while the respective AUCs in serum were not significantly different (30). In addition, Freeman et al. (53) reported a gradual increase in the differences in AUC values obtained from inflammatory and noninflammatory blisters in healthy subjects, from ~3-fold on day 1 to ~30-fold on days 7 to 14. However, the impact of this phagocyte-mediated drug delivery primarily increases the antimicrobial exposure during infection. Once the infection is cleared and tissue homeostasis has been reestablished, the healthy volunteer kinetics outlined in the current paper should hold and may allow a determination of the impact of the terminal elimination kinetics of AZM on resistance development.

It should further be noted that routinely employed pharmacokinetic/pharmacodynamic (PK/PD) indices, such as the $AUC_{0-24}$/MIC ratio, are typically based on a 24-h dosing interval and do not fully account for the consequences that a very long elimination half-life may have on the emergence of resistance. While it is generally accepted that the selective pressure on a given pathogen due to the use of antimicrobial agents changes with increasing drug exposure (cf. inverted-U graphs [54, 55]), the time course of changes in the AUC is typically not taken into consideration. When plotting the number of resistant mutants per ml of growth medium (CFU/ml) versus the $AUC_{0-24}$/MIC ratio, pathogens do not undergo drug-induced selective pressure in the absence of the chemotherapeutic, i.e., at an $AUC_{0-24}$/MIC ratio of zero. As drug exposure (i.e., the $AUC_{0-24}$/MIC ratio) increases, the number of drug-resistant pathogens will also increase. At high $AUC_{0-24}$/MIC ratios, the number of resistant pathogens decreases due to the fact that enough drug is present to kill the pathogen. Once drug treatment is discontinued, AUC values and thus the $AUC_{0-24}$/MIC values decrease to a range in which drug-resistant mutants can survive. The longer the half-life of the drug, the slower the decrease in the $AUC_{0-24}$/MIC ratio, the more time the pathogen will have to adapt to drug-induced selective pressure. This rationale is in line with the finding that the emergence of macrolide-resistant streptococci was more pronounced in healthy volunteers following AZM treatment ($t_{1/2}$, ~68 h) than following treatment with clarithromycin ($t_{1/2}$, ~5 to 7 h) (5). In addition, it is important to realize that the actual shape of the inverted U relies, among other factors, on the following aspects: (i) the presence of resistant mutants at the start of therapy, (ii) the resistance mechanism employed, (iii) the bacterial burden, and (iv) the natural mutation frequency; also, the change in the $AUC_{0-24}$/MIC ratio can be the result of changes in both the $AUC_{0-24}$ and MIC (due to resistant clones), all of which are typically highly interlinked. It has been demonstrated that the probability of selecting preexisting antimicrobial-resistant subpopulations increases with increasing duration of antimicrobial therapy (56). It is consequently important to maximize bacterial kill as early as possible during therapy ("hit hard, hit early" [57]) and to have an antimicrobial agent cleared quickly from the body once treatment is discontinued in order to minimize the probability of creating drug-induced antimicrobial resistance, not only at the primary infection site, but throughout the body. The results of our study indicate that this goal is hard to achieve for AZM due to insufficient early drug exposure in soft tissues and its long residence time at subtherapeutic levels once treatment is discontinued; this leaves three options: (i) increase the dose, at the risk of reaching cytotoxic levels, to achieve maximum initial kill, (ii) give AZM in combination therapy in order to ensure sufficient antimicrobial activity during its long elimination phase, or (iii) do not use the drug, as AZM in and by itself is a resistance generator. Given that AZM has successfully been used for many years for the treatment of respiratory infections, it also showcases the dichotomy between clinical outcome and the emergence of resistance.

In summary, a population PK model was developed for AZM that was able to simultaneously characterize concentrations in plasma, PMLs, and the ISF of muscle and subcutaneous adipose tissue by accounting for differences in ionization at physiological pH values, nonlinear plasma protein binding, and nonspecific tissue binding. The slow release of AZM from the tissues, particularly from PMLs, is responsible for the long terminal half-life of the drug. It is also responsible for maintaining AZM concentrations at subinhibitory levels for a long period of time once drug treatment is discontinued, and it may explain the high rate at which pathogens become macrolide resistant.

## ACKNOWLEDGMENTS

We thank George L. Drusano, Xi-Ling Jiang, and Mirjam Trame for insightful discussions on this project.

We certify that no funding was obtained to perform the research outlined in this article, and we have no conflicts of interest to declare.

## REFERENCES

1. **Peters DH, Friedel HA, McTavish D.** 1992. Azithromycin. A review of its antimicrobial activity, pharmacokinetic properties and clinical efficacy. Drugs **44:**750–799.
2. **Henry DC, Riffer E, Sokol WN, Chaudry NI, Swanson RN.** 2003. Randomized double-blind study comparing 3- and 6-day regimens of azithromycin with a 10-day amoxicillin-clavulanate regimen for treatment of acute bacterial sinusitis. Antimicrob. Agents Chemother. **47:** 2770–2774. http://dx.doi.org/10.1128/AAC.47.9.2770-2774.2003.
3. **Amsden GW.** 1996. Erythromycin, clarithromycin, and azithromycin: are the differences real? Clin. Ther. **18:**56–72; discussion 55. http://dx.doi.org/10.1016/S0149-2918(96)80179-2.
4. **Matzneller P, Krasniqi S, Kinzig M, Sörgel F, Hüttner S, Lackner E, Müller M, Zeitlinger M.** 2013. Blood, tissue, and intracellular concentrations of azithromycin during and after end of therapy. Antimicrob. Agents Chemother. **57:**1736–1742. http://dx.doi.org/10.1128/AAC.02011-12.
5. **Malhotra-Kumar S, Lammens C, Coenen S, Van Herck K, Goossens H.** 2007. Effect of azithromycin and clarithromycin therapy on pharyngeal carriage of macrolide-resistant streptococci in healthy volunteers: a randomised, double-blind, placebo-controlled study. Lancet **369:**482–490. http://dx.doi.org/10.1016/S0140-6736(07)60235-9.
6. **Coles CL, Mabula K, Seidman JC, Levens J, Mkocha H, Munoz B, Mfinanga SG, West S.** 2013. Mass distribution of azithromycin for trachoma control is associated with increased risk of azithromycin-resistant *Streptococcus pneumoniae* carriage in young children 6 months after treatment. Clin. Infect. Dis. **56:**1519–1526. http://dx.doi.org/10.1093/cid/cit137.
7. **Lemaire S, Tulkens PM, Van Bambeke F.** 2010. Cellular pharmacokinetics of the novel biaryloxazolidinone radezolid in phagocytic cells: studies with macrophages and polymorphonuclear neutrophils. Antimicrob. Agents Chemother. **54:**2540–2548. http://dx.doi.org/10.1128/AAC.01723-09.
8. **Foulds G, Shepard RM, Johnson RB.** 1990. The pharmacokinetics of azithromycin in human serum and tissues. J. Antimicrob. Chemother. **25**(Suppl A)**:**73–82.
9. **Crokaert F, Hubloux A, Cauchie P.** 1998. A phase I determination of azithromycin in plasma during a 6-week period in normal volunteers after a standard dose of 500 mg once daily for 3 days. Clin. Drug Invest. **16:**161–166. http://dx.doi.org/10.2165/00044011-199816020-00009.
10. **Kastner U, Guggenbichler JP.** 2001. Influence of macrolide antibiotics on promotion of resistance in the oral flora of children. Infection **29:**251–256. http://dx.doi.org/10.1007/s15010-001-1072-3.

11. **Hahn H, Kaufmann SH.** 1981. The role of cell-mediated immunity in bacterial infections. Rev. Infect. Dis. **3:**1221–1250. http://dx.doi.org/10.1093/clinids/3.6.1221.
12. **Lucchi M, Damle B, Fang A, de Caprariis PJ, Mussi A, Sanchez SP, Pasqualetti G, Del Tacca M.** 2008. Pharmacokinetics of azithromycin in serum, bronchial washings, alveolar macrophages and lung tissue following a single oral dose of extended or immediate release formulations of azithromycin. J. Antimicrob. Chemother. **61:**884–891. http://dx.doi.org/10.1093/jac/dkn032.
13. **Olsen KM, San Pedro GS, Gann LP, Gubbins PO, Halinski DM, Campbell GD, Jr.** 1996. Intrapulmonary pharmacokinetics of azithromycin in healthy volunteers given five oral doses. Antimicrob. Agents Chemother. **40:**2582–2585.
14. **Patel KB, Xuan DW, Tessier PR, Russomanno JH, Quintiliani R, Nightingale CH.** 1996. Comparison of bronchopulmonary pharmacokinetics of clarithromycin and azithromycin. Antimicrob. Agents Chemother. **40:**2375–2379.
15. **Cazzola M, Siniscalchi C, Vinciguerra A, Santangelo G, Matera MG, Rossi F.** 1994. Evaluation of lung tissue and hilar lymph node concentrations of azithromycin. Int. J. Clin. Pharmacol. Ther. **32:**88–91.
16. **Danesi R, Lupetti A, Barbara C, Ghelardi E, Chella A, Malizia T, Senesi S, Angeletti CA, Del Tacca M, Campa M.** 2003. Comparative distribution of azithromycin in lung tissue of patients given oral daily doses of 500 and 1000 mg. J. Antimicrob. Chemother. **51:**939–945. http://dx.doi.org/10.1093/jac/dkg138.
17. **Harrison JD, Jones JA, Morris DL.** 1991. Azithromycin levels in plasma and gastric tissue, juice and mucus. Eur. J. Clin. Microbiol. Infect. Dis. **10:**862–864. http://dx.doi.org/10.1007/BF01975843.
18. **Schmaljohann D.** 2006. Thermo- and pH-responsive polymers in drug delivery. Adv. Drug Deliv. Rev. **58:**1655–1670. http://dx.doi.org/10.1016/j.addr.2006.09.020.
19. **Satchell L, Leake DS.** 2012. Oxidation of low-density lipoprotein by iron at lysosomal pH: implications for atherosclerosis. Biochemistry **51:**3767–3775. http://dx.doi.org/10.1021/bi2017975.
20. **Bouvier d'Yvoire MJ, Dresco IA, Tulkens PM.** 1998. Computer-aided prediction of macrolide antibiotic concentrations in human circulating polymorphonuclear leucocytes. J. Antimicrob. Chemother. **41**(Suppl B)**:** 63–68.
21. **Montenez JP, Van Bambeke F, Piret J, Schanck A, Brasseur R, Tulkens PM, Mingeot-Leclercq MP.** 1996. Interaction of the macrolide azithromycin with phospholipids. II. Biophysical and computer-aided conformational studies. Eur. J. Pharmacol. **314:**215–227.
22. **Van Bambeke F, Montenez JP, Piret J, Tulkens PM, Courtoy PJ, Mingeot-Leclercq MP.** 1996. Interaction of the macrolide azithromycin with phospholipids. 1. Inhibition of lysosomal phospholipase A1 activity. Eur. J. Pharmacol. **314:**203–214.
23. **Trapp S, Rosania GR, Horobin RW, Kornhuber J.** 2008. Quantitative modeling of selective lysosomal targeting for drug design. Eur. Biophys. J. **37:**1317–1328. http://dx.doi.org/10.1007/s00249-008-0338-4.
24. **Rodgers T, Leahy D, Rowland M.** 2005. Physiologically based pharmacokinetic modeling 1: predicting the tissue distribution of moderate-to-strong bases. J. Pharm. Sci. **94:**1259–1276. http://dx.doi.org/10.1002/jps.20322.
25. **Ohkuma S, Poole B.** 1978. Fluorescence probe measurement of the intralysosomal pH in living cells and the perturbation of pH by various agents. Proc. Natl. Acad. Sci. U. S. A. **75:**3327–3331. http://dx.doi.org/10.1073/pnas.75.7.3327.
26. **Carlier MB, Garcia-Luque I, Montenez JP, Tulkens PM, Piret J.** 1994. Accumulation, release and subcellular localization of azithromycin in phagocytic and non-phagocytic cells in culture. Int. J. Tissue React. **16:** 211–220.
27. **Steinman RM, Brodie SE, Cohn ZA.** 1976. Membrane flow during pinocytosis. A stereologic analysis. J. Cell Biol. **68:**665–687.
28. **Aubert-Tulkens G, Van Hoof F, Tulkens P.** 1979. Gentamicin-induced lysosomal phospholipidosis in cultured rat fibroblasts. Quantitative ultrastructural and biochemical study. Lab. Invest. **40:**481–491.
29. **de Duve C, de Barsy T, Poole B, Trouet A, Tulkens P, Van Hoof F.** 1974. Commentary. Lysosomotropic agents. Biochem. Pharmacol. **23:** 2495–2531. http://dx.doi.org/10.1016/0006-2952(74)90174-9.
30. **Ballow CH, Amsden GW, Highet VS, Forrest A.** 1998. Pharmacokinetics of oral azithromycin in serum, urine, polymorphonuclear leucocytes and inflammatory vs non-inflammatory skin blisters in healthy volunteers. Clin. Drug Invest. **15:**159–167. http://dx.doi.org/10.2165/00044011-199815020-00009.
31. **Amsden GW, Nafziger AN, Foulds G.** 1999. Pharmacokinetics in serum and leukocyte exposures of oral azithromycin, 1,500 milligrams, given over a 3- or 5-day period in healthy subjects. Antimicrob. Agents Chemother. **43:**163–165.
32. **Homma T, Fujimura T, Maki H, Yamano Y, Shimada J, Kuwahara S.** 2010. *In vitro* antibacterial activities of S-013420, a novel bicyclolide, against respiratory tract pathogens. J. Antimicrob. Chemother. **65:**1433–1440. http://dx.doi.org/10.1093/jac/dkq147.
33. **Boucher HW, Talbot GH, Bradley JS, Edwards JE, Gilbert D, Rice LB, Scheld M, Spellberg B, Bartlett J.** 2009. Bad bugs, no drugs: no ESKAPE! An update from the Infectious Diseases Society of America. Clin. Infect. Dis. **48:**1–12. http://dx.doi.org/10.1086/595011.
34. **Bell BG, Schellevis F, Stobberingh E, Goossens H, Pringle M.** 2014. A systematic review and meta-analysis of the effects of antibiotic consumption on antibiotic resistance. BMC Infect. Dis. **14:**13. http://dx.doi.org/10.1186/1471-2334-14-13.
35. **Valery PC, Morris PS, Byrnes CA, Grimwood K, Torzillo PJ, Bauert PA, Masters IB, Diaz A, McCallum GB, Mobberley C, Tjhung I, Hare KM, Ware RS, Chang AB.** 2013. Long-term azithromycin for indigenous children with non-cystic-fibrosis bronchiectasis or chronic suppurative lung disease (Bronchiectasis Intervention Study): a multicentre, double-blind, randomised controlled trial. Lancet Respir. Med. **1:**610–620. http://dx.doi.org/10.1016/S2213-2600(13)70185-1.
36. **Hare KM, Singleton RJ, Grimwood K, Valery PC, Cheng AC, Morris PS, Leach AJ, Smith-Vaughan HC, Chatfield M, Redding G, Reasonover AL, McCallum GB, Chikoyak L, McDonald MI, Brown N, Torzillo PJ, Chang AB.** 2013. Longitudinal nasopharyngeal carriage and antibiotic resistance of respiratory bacteria in indigenous Australian and Alaska native children with bronchiectasis. PLoS One **8:**e70478. http://dx.doi.org/10.1371/journal.pone.0070478.
37. **Li H, Liu DH, Chen LL, Zhao Q, Yu YZ, Ding JJ, Miao LY, Xiao YL, Cai HR, Zhang DP, Guo YB, Xie CM.** 2014. Meta-analysis of the adverse effects of long-term azithromycin use in patients with chronic lung diseases. Antimicrob. Agents Chemother. **58:**511–517. http://dx.doi.org/10.1128/AAC.02067-13.
38. **Montenez JP, Van Bambeke F, Piret J, Schanck A, Brasseur R, Tulkens PM, Mingeot-Leclercq MP.** 1996. Interaction of the macrolide azithromycin with phospholipids. II. Biophysical and computer-aided conformational studies. Eur. J. Pharmacol. **314:**215–227.
39. **Pillay J, den Braber I, Vrisekoop N, Kwast LM, de Boer RJ, Borghans JA, Tesselaar K, Koenderman L.** 2010. *In vivo* labeling with $2H_2O$ reveals a human neutrophil lifespan of 5.4 days. Blood **116:**625–627. http://dx.doi.org/10.1182/blood-2010-01-259028.
40. **Craig WA.** 1998. Pharmacokinetic/pharmacodynamic parameters: rationale for antibacterial dosing of mice and men. Clin. Infect. Dis. **26:**1–10, quiz 11–12. http://dx.doi.org/10.1086/516284.
41. **Nightingale CH.** 1997. Pharmacokinetics and pharmacodynamics of newer macrolides. Pediatr. Infect. Dis. J. **16:**438–443. http://dx.doi.org/10.1097/00006454-199704000-00027.
42. **Jacobs MR, Bajaksouzian S, Zilles A, Lin G, Pankuch GA, Appelbaum PC.** 1999. Susceptibilities of *Streptococcus pneumoniae* and *Haemophilus influenzae* to 10 oral antimicrobial agents based on pharmacodynamic parameters: 1997 U.S. surveillance study. Antimicrob. Agents Chemother. **43:**1901–1908.
43. **Schentag JJ, Ballow CH.** 1991. Tissue-directed pharmacokinetics. Am. J. Med. **91:**5S–11S. http://dx.doi.org/10.1016/0002-9343(91)90394-D.
44. **Amsden GW.** 2001. Advanced-generation macrolides: tissue-directed antibiotics. Int. J. Antimicrob. Agents **18**(Suppl 1)**:**S11–S15. http://dx.doi.org/10.1016/S0924-8579(01)00410-1.
45. **Bonnet M, Van der Auwera P.** 1992. *In vitro* and *in vivo* intraleukocytic accumulation of azithromycin (CP-62, 993) and its influence on *ex vivo* leukocyte chemiluminescence. Antimicrob. Agents Chemother. **36:**1302–1309. http://dx.doi.org/10.1128/AAC.36.6.1302.
46. **Wildfeuer A, Laufen H, Müller-Wening D, Haferkamp O.** 1989. Interaction of azithromycin and human phagocytic cells. Uptake of the antibiotic and the effect on the survival of ingested bacteria in phagocytes. Arzneimittelforschung **39:**755–758.
47. **Hand WL, Hand DL.** 2001. Characteristics and mechanisms of azithromycin accumulation and efflux in human polymorphonuclear leukocytes. Int. J. Antimicrob. Agents **18:**419–425. http://dx.doi.org/10.1016/S0924-8579(01)00430-7.

48. **Gladue RP, Snider ME.** 1990. Intracellular accumulation of azithromycin by cultured human fibroblasts. Antimicrob. Agents Chemother. **34:**1056–1060. http://dx.doi.org/10.1128/AAC.34.6.1056.
49. **Hoepelman IM, Schneider MM.** 1995. Azithromycin: the first of the tissue-selective azalides. Int. J. Antimicrob. Agents **5:**145–167. http://dx.doi.org/10.1016/0924-8579(95)00009-W.
50. **Lardner A.** 2001. The effects of extracellular pH on immune function. J. Leukoc. Biol. **69:**522–530.
51. **Grinstein S, Swallow CJ, Rotstein OD.** 1991. Regulation of cytoplasmic pH in phagocytic cell function and dysfunction. Clin. Biochem. **24:**241–247. http://dx.doi.org/10.1016/0009-9120(91)80014-T.
52. **Lucini, V, Grosso S, Pannacci M, Scaglione F.** Azithromycin kinetics in infected tissue evaluated by microdialysis, abstr. A-335. 46th Intersci. Conf. Antimicrob. Agents Chemother. (ICAAC), San Francisco, CA, 27 to 30 September 2006.
53. **Freeman CD, Nightingale CH, Nicolau DP, Belliveau PP, Banevicius MA, Quintiliani R.** 1994. Intracellular and extracellular penetration of azithromycin into inflammatory and noninflammatory blister fluid. Antimicrob. Agents Chemother. **38:**2449–2451. http://dx.doi.org/10.1128/AAC.38.10.2449.
54. **Tam VH, Louie A, Deziel MR, Liu W, Leary R, Drusano GL.** 2005. Bacterial-population responses to drug-selective pressure: examination of garenoxacin's effect on *Pseudomonas aeruginosa*. J. Infect. Dis. **192:**420–428. http://dx.doi.org/10.1086/430611.
55. **Tam VH, Louie A, Deziel MR, Liu W, Drusano GL.** 2007. The relationship between quinolone exposures and resistance amplification is characterized by an inverted U: a new paradigm for optimizing pharmacodynamics to counterselect resistance. Antimicrob. Agents Chemother. **51:**744–747. http://dx.doi.org/10.1128/AAC.00334-06.
56. **Jumbe N, Louie A, Leary R, Liu W, Deziel MR, Tam VH, Bachhawat R, Freeman C, Kahn JB, Bush K, Dudley MN, Miller MH, Drusano GL.** 2003. Application of a mathematical model to prevent *in vivo* amplification of antibiotic-resistant bacterial populations during therapy. J. Clin. Invest. **112:**275–285. http://dx.doi.org/10.1172/JCI200316814.
57. **Ehrlich P.** 1913. Address in pathology on chemotherapeutics: scientific principles, methods, and results. Lancet **ii:**445–451.